

Toward a Real-Time Tracking of a Medical Deformable Needle from Strain Measurements

A.L.G Robert, G. Chagnon, A. Bonvilain, P. Cinquin and A. Moreau-Gaudry

Abstract— Needles used in medical percutaneous procedures are brought to deform because of its interactions with inhomogeneous and anisotropic tissues. In this paper, the first step of the development of a new generation of tools for assistance in the realization of gestures taking into account these deformations are presented. We provide a new approach for determining, in “real time” and in 3D, the shape of an instrumented needle inserted into a complex tissue by using strain microgauges. The knowledge of the real time local deformation from these strain microgauges would improve the current navigation systems by considering not only the rigid needles but also the flexible ones. Our aim is to reconstruct in real time the instrumented needle shape in order to help tracking and steering during a medical intervention.

I. INTRODUCTION

Within the framework of medical percutaneous procedures based on the insertion of needles, the access for the clinician to a new needle navigation system could further optimize the procedures accuracy [1].

Many techniques were developed to assist in the realization of gestures. These techniques are specific of each method of imagery used (CT scan (Computerized Tomography), magnetic resonance imaging (MRI), ultrasound) for real-time or only preoperative imaging and are very largely carried out in a daily way. Nevertheless, such strategies are limited due to the position inaccuracy coming from the needle deflection during a percutaneous procedure. Furthermore, the effectiveness of imaging are restricted because of the limited detectable depth resulting from the loss of ultrasound propagation with poor image quality, the radiation exposure in X-ray with insufficient image quality and the incompatibility of some metallic instruments to the magnetic field.

While the medical imaging is constantly improving with ever finer spatial resolutions, the tools available to the radiologist to guide and locate themselves in real time in the images remain rather few developed to date. They may involve the use of robotic [2], optical ([3], [4]) or electromagnetic ([5], [6]) devices. Such strategies suffer from major limitations in their application to the

interventional radiology, among which the assumption of the non-deformability and the difficulty of steering the used tool. A significant among of work has been dealing with the navigation system of flexible needles. Di Maio and Salcudean [7] introduced a new motion planning approach for the insertion of flexible needles into soft tissues based on numerical models using potential fields, in order to guide the needle tip to a target, avoiding the obstacles. Glozman and Shoham [8] proposed a model of a flexible needle and of the tissue forces on it following the insertion as a linear beam supported by virtual springs and. Through the solution of the forward and inverse kinematics of the needle, they provided a simulation and path planning in real-time. Chan et al. [9] proposed a tracking device for monitoring the location and the orientation of a needle with respect to an ultrasound probe, using a system of two cameras.

Regardless of the strategy used, taking into account the needle deflection and then tracking the needle to assist in the realization of gestures could further make the procedure:

- Safer because the position and the deflection of the needle would be better known in real time without any additional imagery throughout the procedure.
- Less invasive because the number of attempts needed for the placement of a needle, which does not follow the planned trajectory, could be decreased. Moreover, the number of controls to ensure the correct positioning of the needle and thus the amount of irradiation received by patients and medical staff during CT-guided could be reduced.
- More efficient because of better positioning of the needle tip at its target.

The model associated with the reconstruction of the needle starting from the information given by the strain microgauges with the first associated 2D/3D results is presented here.

II. METHODS

A. Strain microgauges

Works in progress raise the problems to incorporate strain microgauges on the needle. These microgauges inform on the local deformations of the needle as shown in equation 1.

$$\frac{\Delta R_{\varepsilon}}{R_{\varepsilon}} = k \frac{\Delta L}{L} = k\varepsilon \quad (1)$$

A.L.G. Robert (corresponding author) , P. Cinquin, A. Moreau-Gaudry are with the TIMC-IMAG Laboratory (CNRS-UJF), Domaine de la Merci, La Tronche 38706 France (phone: +33456520004; e-mail: Adeline.Robert@imag.fr, Alexandre.Moreau-Gaudry@imag.fr).

G. Chagnon is with the 3SR Laboratory (CNRS-UJF-Grenoble INP), Domaine Universitaire, BP 53, Grenoble Cedex9 38041 France.

A. Bonvilain is with the TIMA Laboratory (CNRS-UJF-Grenoble INP), 46 Avenue Felix Viallet, Grenoble Cedex1 38031 France.

Where R_e is the electrical resistance, ε is the relative variation of length and k the sensitivity of the microgauge.

A state of the art on the various fields concerned with the realization of a passive needle (guidance of the medical tools, deformation measurements) was recently carried out [10] and showed that no approach is currently planned to acquire local information of deformation starting from micro sensors integrated on a cylindrical substrate of low diameter.

The way of the micro-fabrication is preferred [10], which uses manufacturing process resulting from the microelectronics. The first achievements of micro-fabrication allowed verifying experimentally the feasibility to incorporate strain microgauges on the needle as shown in fig. 1.

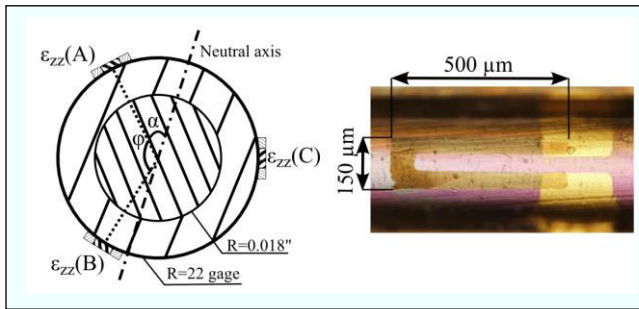


Figure 1. Schematic layout of the strain microgauges and deposit of a strain microgauge on a steel needle by micro-fabrication.

The micro-fabrication of microgauges highlights a limit of the possible number of positions accepted not to interfere with connections. Indeed the microgauges are connecting to an instrumentation circuit and a PCI-6221 data acquisition board.

In this work, it was decided to use three microgauges in a same section with an angle of $\varphi=120^\circ$ (Fig. 1). The information from these three microgauges was studied and is presented below.

B. Relation between strain microgauges and Beam Theory

Needles can be considered as mono-dimensional structures (as beam element) as the length of the neutral axis is large compared to the dimensions of the cross-sections.

The following two assumptions are also true for needles:

- The radius of curvature of the neutral axis is large compared to the cross-sections dimensions.
- The possible variations of the surface of the cross-section are weak and progressive.

The needle being brought to deform, it will be supposed that:

- The deformations undergone by the needle, as well as the displacements which can be measured, remain small (small deformation assumption) so that the solid remains in the elastic domain.
- The points of external load application remain constant throughout.

Based on these hypotheses, the bending moment-curvature beam equation can therefore be written as:

$$\gamma \approx \frac{d^2y}{dx^2} = \frac{M_f}{EI} = \frac{\varepsilon}{r} \quad (2)$$

Where γ is the curvature of the needle, y is the displaced position of the needle, x is the coordinate along the beam, M_f is the bending moment, E is the Young's modulus of the material, I is the second moment of area and r the distance between the microgauges and the neutral axis.

Furthermore, it is possible to determine the curvature of a needle in 3D using strain microgauges as shown in fig. 2.

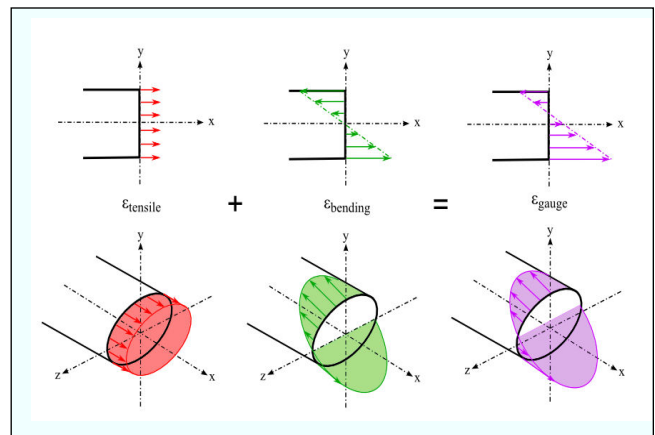


Figure 2. Superposition principle of a deformable needle.

Strain microgauges take into account the bending and tensile deformations:

$$\varepsilon_{gauge} = \varepsilon_{tensile} + \varepsilon_{bending} \quad (3)$$

With:

$$\varepsilon_{bending} = \frac{M_f}{EI} \times R \sin \alpha \quad (4)$$

The complete information from the strain microgauges is:

$$\begin{aligned} \varepsilon_{zz}^T(A) &= \varepsilon_{tensile} + R \sin \alpha \\ \varepsilon_{zz}^T(B) &= \varepsilon_{tensile} + R \sin(\alpha + \varphi) \\ \varepsilon_{zz}^T(C) &= \varepsilon_{tensile} + R \sin(\alpha + 2\varphi) \end{aligned} \quad (5)$$

Where φ is the angle between two microgauges (Fig. 1), R is the radius of the needle and α is the angle between the neutral axis and a microgauge.

The tensile deformation can be determined and then it can be remove to only take into account the bending deformation. This deformation can be used to determine the curvature of the needle (γ) and the neutral axis (α) according to the Beam theory:

$$\tan \alpha = -\sqrt{3} \frac{\varepsilon_{zz}(B) + \varepsilon_{zz}(C)}{\varepsilon_{zz}(B) - \varepsilon_{zz}(C)}$$

$$\gamma \approx \frac{M_f}{EI} = \frac{2}{\sqrt{3}R} \sqrt{\varepsilon_{zz}(B)^2 + \varepsilon_{zz}(C)^2 + \varepsilon_{zz}(B)\varepsilon_{zz}(C)}$$
(6)

C. Needle model

Needle deflections were approximated as a uniform cubic B-spline S, i.e. as a linear combination of basis cubic B-splines ([11], [12]). A regular grid of $n+1$ real values t_i ($i=0\dots n$, with $n=6$ in this study), called knots with $0=t_0<\dots<t_n=L$ (with L the length of the needle), was defined and the expression of S was:

$$\forall t \in [t_0, t_n], S(t) = \sum_{i=-3}^{n-1} P_i N_{i,k}(t)$$
(7)

Where $k=3$ is the degree of the B-spline, P_i are the control points for the needle deflection and $N_{i,k}$ are the B-splines base. Each are determined starting from the preceding ones by recurrence.

The P_i coefficients were totally defined by minimizing the following problem:

$$u_0(S(0) - y_0)^2 + u_1(S'(0) - dy_0)^2 + \sum_{k=1}^m w_k(S''(x_k) - y''_k)^2 + \tau \int_0^L S^{(3)}(t)^2 dt$$
(8)

Where ($'$, $''$, $'''$) represent the first three derivatives. (x_k , y''_k), $k=1\dots m$ are the microgauges information (position and bending) with m the number of microgauges, y_0 and dy_0 are the information on the position and the orientation of the proximal extremity, u_0 , u_1 , w_k and τ are the weights chosen to acquire a good compromise between the smoothness of the result and the interpolated cubic B-spline.

III. RESULTS AND DISCUSSION

To test the performance of the proposed model and without a prototype usable at present, we simulated the microgauges information from real clinical needles (Fig. 3) and virtual needles. The choice of 2 positions was made in order to response to the micro fabrication problem. This corresponds to two sections of three microgauges. The optimal positions of the strain microgauges are determined using a minimization algorithm. It attempts to find a constrained minimum of a scalar function (starting from

information previously established [13]) of several variables starting at an initial estimate.

Information of virtual microgauges was simulated and used as input to reconstruct the needle with Matlab (Version 7.11.0.584). A personal computer with an Intel® Core™ i7-2600 3GHz processor and 7 GB of RAM was used to make these simulations. The calculation time for the needle reconstruction starting from microgauges information is shown in Table 1 following the number of sections carrying microgauges.

An example of reconstruction of a real clinical needle is shown in fig. 3 with its 2D projections. The tip reconstruction errors in the two projection planes, for the needle of 200mm length, are 0.4mm and 0.7mm, respectively.

The desired tolerance for the accuracy of needle insertion in percutaneous procedures depends on the application and is not well-defined general information. However, millimeter accuracy can be required in procedures such as biopsies [14]. This approach of tracking may be compatible with the clinical practice.

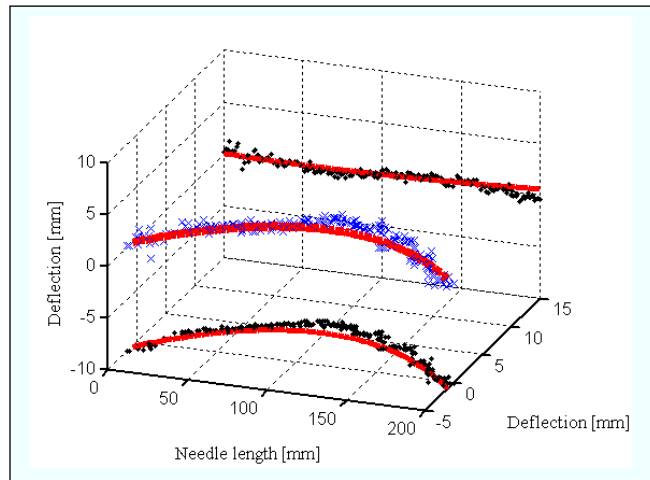


Figure 3. 3D reconstruction of a medical needle from two local strain measurements (6 microgauges).

A work on the parameters of the model must be carried out to find the best compromise of reconstruction on a set of representative needles of the real procedures. A future work will also be made with a real time prototype.

IV. CONCLUSION

In this paper, we studied the feasibility of reconstructing, with an instrumented needle, the 3D deflection of this one. By using static Beam and B-spline theories and the information given by the strain microgauges incorporated on the needle, the 3D needle shape can be determined. To minimize positioning error and post-operative complications during percutaneous procedures, it is important to be able to track in real time any tool deviation from the planned trajectory.

TABLE I. EXAMPLE OF CALCULATION TIME FOR SEVERAL NEEDLE RECONSTRUCTION FOLLOWING THE NUMBER OF MICROGAUGES

Needles	Numbers of sections / Number of microgauges		
	1/3	2/6	3/9
N°1	1.820 μ sec	1.828 μ sec	1.840 μ sec
N°2	1.802 μ sec	1.817 μ sec	1.848 μ sec

V. ACKNOWLEDGMENT

This work was supported by French state funds managed by the ANR within the Investissements d’Avenir programme (Labex CAMI) under the reference ANR-11-LABX-0004 and by the ANR Tecsan (project GAME-D) under reference ANR-GUI-AAP-05.

REFERENCES

- [1] Moreau-Gaudry, A., Bonvilain, A., Basrou, S, Cinquin, P., 2008. Medical Needles Deformation Tracking. Medical Image Computing and Computer-Assisted Intervention MICCAI workshop 2008.
- [2] Hungr, N., Fouard, C., Robert, A., Bricault, I., Cinquin, P., 2011. Interventional radiology robot for CT and MRI-guided guided percutaneous interventions. Medical Image Computing and Computer-Assisted Intervention MICCAI 2011, pp.137-144.
- [3] Park, Y., Elayaperumal, S., Daniel, B., Ryu, S., Shin, M., Savall, J., Black, R., Moslehi, B., Cutkosky, M., 2010. Real-time estimation of 3-d needle shape and deflection for MRI-guided interventions. IEEE/ASME Transactions on Mechatronics, vol.15(6), pp.906-915.
- [4] Desjardins, A., van~der Voort, M., Roggeveen, S., Lucassen, G., Bierhoff, W., Hendriks, B., Brynolf, M., Holmstr{\v{o}}m, B., 2011. Needle stylet with integrated optical fibers for spectroscopic contrast during peripheral nerve blocks. Journal of Biomedical Optics, vol.16, pp.077004.
- [5] Hushek, S., Fetics, B., Moser, R., Hoerter, N., Russell, L., Roth, A., Polenur, D., Nevo, E., Hushek, S., 2004. Initial clinical experience with a passive electromagnetic 3D locator system. 5th Interventional MRI Symposium, pp.73-74.
- [6] Lei, P., Moeslein, F., Wood, B., Shekhar, R., 2011. Real-time tracking of liver motion and deformation using a flexible needle. CARS, vol.6, pp.435-446.
- [7] DiMaio, Salcudean, 2003. Needle steering and model based trajectory planning. MICCAI, vol.2878, pp.33-44.
- [8] Glozman, Daniel and Shoham, Moshe, 2004. Flexible needle steering and optimal trajectory planning for percutaneous therapies. MICCAI, vol. 3217, pp.137-144.
- [9] Chan, Candice and Lam, Felix and Rohling, Robert, 2005. A needle tracking device for ultrasound guided percutaneous procedures. Ultrasound in medicine & biology, vol.31, pp.1468-1483.
- [10] Yang, W., Bonvilain, A., Alonso,T., Moreau-Gaudry, A., Basrou, S., 2010. Modelling and characterization of an instrumented medical needle in sight of new microsensor design for its insertion guidance. EMBC, pp.6465-6468.
- [11] De Boor, C., 1978. A practical guide to splines. Springer.
- [12] Laurent, P.J., Le Méhauté, A., Schumaker, L.L., 1991. Curves and surfaces. Academic Press.
- [13] Robert, A.L.G., Chagnon, G., Bricault, I., Cinquin, P., Moreau-Gaudry, A., 2013. A Generic Three Dimensional Force Distribution Basis Applied to a Surgical Needle Inserted into a Complex Tissue. Submitted to the Journal of the Mechanical Behavior of Biomedical Materials.
- [14] Van Gerwen, D., Dankelman, J., Van den Dobbelsteen, J., 2012. Needle-tissue interaction forces-a survey of experimental data. Medical engineering & Physics, vol.34 (6), pp.665-680.